ELSEVIER

NUCLEAR PHYSICS A

^{130}Te and ^{128}Te double beta decay half-lives

A.P. Meshik [a,*], C.M. Hohenberg [a], O.V. Pravdivtseva [a],
T.J. Bernatowicz [a], Y.S. Kapusta [b]

[a] *Laboratory for the Space Sciences and Physics Department, Washington University,
CB1105, One Brookings Drive, Saint Louis, MO 63130, USA*
[b] *Activation Laboratories LTD, 1336 Sandhill Drive, Ancaster, ON, L9G 4V5, Canada*

Abstract

The double beta decay half-lives of ^{130}Te measured in geological Te specimens of known age fall into two distinct groups: $2.5 \pm 0.4 \times 10^{21}$ yr and $8 \pm 1 \times 10^{20}$ yr. Discussion about which value is correct has lasted for more than 30 years without a satisfactory resolution. Since the ratio of the ^{130}Te half-life to that of ^{128}Te is known ($3.74 \pm 0.11 \times 10^{-4}$), the ^{128}Xe half-life, which constrains the effective Majorana mass of the neutrino, also becomes uncertain within this factor of ~ 3. Here we describe several experiments and observations, which lead us to the conclusion that the "short" half-lives are more likely to be correct. This is in agreement with preliminary results recently obtained in the direct counting NEMO-3 experiment.
© 2008 Elsevier B.V. All rights reserved.

Keywords: RADIOACTIVITY ^{128,130}Te($\beta\beta$); analyzed half-life of geological samples

1. Introduction

The determination of the double beta decay half-life (DBDHL) of ^{130}Te $\rightarrow$ ^{130}Xe using geological samples of known age is based on the ^{130}Xe/^{130}Te ratio measured in Te-bearing minerals, native (metallic) Te and tellurides, assuming complete retention of the Xe daughter. The first measurement of the ^{130}Te DBDHL was made 58 years ago by Ingram and Reynolds [1]. Since then, numerous determinations, performed in different laboratories using tellurium min-
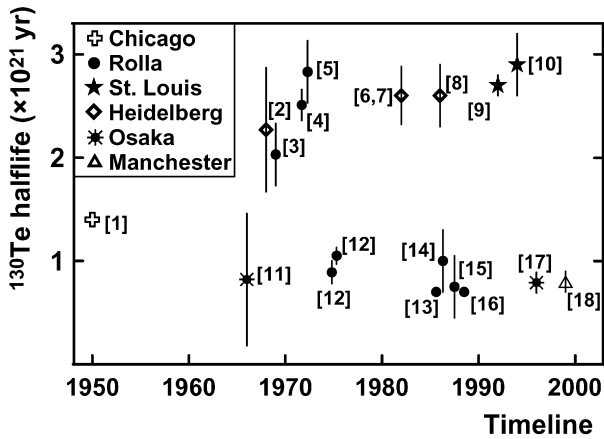

Fig. 1. Half-lives of ^{130}Te double beta decay measured in geological Te samples tend to form two distinct groups.

erals of different ages, have yielded ^{130}Te DBDHLs that tend to fall into two distinct groups, $2.5 \pm 0.4 \times 10^{21}$ yr [2–10] and $8 \pm 1 \times 10^{20}$ yr [11–18], which clearly differ substantially more than the experimental uncertainties (Fig. 1).

Different research groups advocating for either the "low" or "high" DBDHL values have suggested two explanations. High DBDHL proponents have suggested that "parentless" radiogenic ^{130}Xe may have been trapped during telluride formation in the same way that the well-known "parentless" ^{40}Ar is sometimes inherited from earlier generation K-minerals, making the DB-DHL artificially short and consequently unreliable. On the other hand, low DBDHL proponents have proposed diffusive losses of radiogenic ^{130}Xe. The large atomic radius of Xe makes thermal diffusion unlikely under normal thermal conditions, especially in metals. This is demonstrated in the quantitative retention of ^{129}Xe for 4.6 billion years in I–Xe dating but, if diffusive losses do occur, the lower values for the half-life would represent only an upper limit of the true ^{130}Te DBDHL. However, no experiments have been carried out to either verify or rule out either of these arguments. Discussion about which value of the ^{130}Te DBDHL is correct has lasted for more than 3 decades and the low and high DBDHLs still coexist in the literature. It was noted that, as a rule, young (~ 100 Myr) samples yield ^{130}Te DBDHL lower than the old (> 1 Gyr) ones. From this observation, it was proposed that perhaps both the long and short ^{130}Te DB-DHL may be correctly measured but that the observed difference may be due to variability of Fermi constant, G_F^4, with time [19,20]. We will dismiss this possibility for the simple reason that, if the weak interaction constant does indeed depend on time, it must not be unique to Te decay, and there is no evidence for such a temporal effect in other electro-weak decay rates. For instance, there is very good agreement between the "present" ^{82}Se DBDHL, measured by counting in the MEMO experiment [21] and those measured by daughter accumulation in geological Se samples from the 4.5 Ga old Cape York meteorite [22] and other samples of intermediate age [23].

The unresolved controversy of ^{130}Te DBDHL compromises the entire "geochemical" approach (a widespread, somewhat misleading term), promoting skepticism in the results obtained from other geological samples, for example, the first and only positive experimental evidence for Double Electron Capture in ^{130}Ba [24]. The goal of this work is to quantitatively examine arguments of both low and high DBDHL proponents, to perform the appropriate diagnostic experiments in an attempt to delineate the cause for half-life discordance and to determine which

group of ages is valid. We report here the results of these experiments, designed and conducted specifically to determine (1) whether ^{130}Xe in tellurium minerals has parentless contributions from inherited excesses and (2) whether significant ^{130}Xe has been lost from Te minerals during geological storage.

2. Evaluation of inherited ^{130}Xe

The most suitable samples for this experiment are relatively young tellurides formed by late-stage hydrothermal Te deposition during which inherited ^{130}Xe could have been acquired from the surrounding hosts or from the aqueous medium. Native tellurium from the Kochbulak gold–tellurium deposit in Uzbekistan is ideally suited for this experiment since "the Kochbulak deposit was formed during the cyclic multistage process..." [25]. Geological and paleographical studies of this area set limits for ore formation between 61 and 89 Myr [26].

The Kochbulak tellurium sample was kindly provided by Dr. V.A. Kovalenker (Russian Academy of Sciences). It consisted of several 10–30 mg fragments, none of which demonstrated any signs of oxidation or visible inclusions. We therefore assume that it is pure metallic Te, although for this particular experiment, purity is not required. The sample was placed into an ultra-high vacuum extraction furnace where it was subjected to step-wise pyrolysis. Gases evolved at each extraction temperatures were subsequently cleaned from the chemically active components using SEAS 707 Ti–Zr–Al getters and freshly deposited Ti film. He, Ne, Ar and most of the Kr were removed by cryogenic separation on activated charcoal. The purified Xe was then analyzed in the high sensitivity ion-counting mass spectrometer used for measurement of $\beta\beta$-decays of Ba and Te isotopes previously reported [24,27].

The Kochbulak sample was at least 99% metallic Te and, by summing all temperature fractions (Table 1) we determined the ^{130}Xe/Te ratio to be 10.5×10^{-12} cm^3 STP/g, implying a ^{130}Te half-life between 2.4 and 3.5×10^{20} yr, significantly lower than even the "low" DBDHL values shown in Fig. 1. If this sample were less than 99% metallic Te the apparent half-life would be even smaller so there is a good chance that some extra ^{130}Xe from the previous generation of Te-ores could be present. A similar value (3.3×10^{20} yr) was obtained earlier from the 743 Myr old Kalgoorlie krennerite (best estimate from [9]), where the authors concluded that this low value must be due to the "inheritance of ^{130}Xe from older Te ores" [27]. These two self-consistent samples, therefore, seem optimal for the search of potential ^{130}Xe inherited excesses.

To examine whether "parentless" ^{130}Xe contributions are, indeed, present, we investigated the correlations between $\beta\beta$-decay ^{130}Xe and Xe produced by the reactions of ^{128}Te and ^{130}Te with natural neutrons produced by cosmic ray muons and/or actinide fission. "Parentless" inherited excesses of ^{130}Xe should not be uniformly distributed within the native Te sample and thus should not correlate with ^{131}Xe and/or ^{129}Xe produced by neutron capture on ^{128}Te and ^{130}Te. Indeed, there are well-defined linear correlations between ^{129}Xe/^{132}Xe, ^{131}Xe/^{132}Xe and ^{130}Xe/^{132}Xe released from these two samples during a step-wise heating experiment (Fig. 2a). Although differing in slope due to different neutron fluences, energy spectra and perhaps incomplete decay of intermediate ^{129}I, straight mixing lines observed for both ratios indicate that only two components are present: Xe derived from Te and "trapped" Xe of atmospheric composition that pre-existed in the sample. There is no evidence for a third component that is not correlated with the Te itself. In other words, the two components expected (Te-produced and trapped Xe) are the two end-members, present in different proportions at different extraction temperatures which provide straight mixing lines. Inherited ^{130}Xe, if present in measurable quantities, should be visible as departures from the lines or, if it was previously homogenized with trapped Xe,

Table 1

Concentration and isotopic composition of xenon (^{130}Xe $\equiv$ 100) released from 149.9 mg Kochbulak native tellurium (Uzbekistan) during stepwise pyrolysis. Shown uncertainties are 1σ (68% CL). Concentration of ^{130}Xe is accurate to $\sim 7\%$ due to variations of absolute sensitivity of the mass spectrometer. Numbers in the second line are corrected for air contamination assuming all ^{132}Xe is atmospheric, i.e. ^{130}Te solely from $\beta\beta$ decay

Temp. (°C)[a]	^{130}Xe (10^{-12} cm³ STP/g)[b]	^{124}Xe	^{126}Xe	^{128}Xe	^{129}Xe	^{131}Xe	^{132}Xe	^{134}Xe	^{136}Xe
250	0.038	1.42 ± 0.94	2.70 ± 1.09	42.96 ± 2.93	534 ± 23	492 ± 29	598 ± 31	255 ± 12	230 ± 11
	0.004	-72 ± 11.6	7.5 ± 11.5	4.2 ± 36.8	-558 ± 630	206 ± 337	0.00 ± 450	244 ± 129	340 ± 125
300	0.142	1.54 ± 0.60	0.75 ± 0.62	13.3 ± 2.1	191 ± 13	182.4 ± 14.5	192 ± 14	52.8 ± 8.3	43.9 ± 7.7
	0.101	1.21 ± 0.81	0.17 ± 0.88	-0.54 ± 3.25	4 ± 27	43 ± 25	0.00 ± 28	-30 ± 15	-27 ± 13
330	0.533	0.04 ± 0.17	0.03 ± 0.21	2.67 ± 0.79	51.0 ± 4.7	52.4 ± 6.9	35.1 ± 3.5	13.2 ± 2.1	10.6 ± 3.0
	0.505	-0.48 ± 0.18	-0.08 ± 0.23	0.18 ± 0.87	17.4 ± 6.1	26 ± 8	0.00 ± 5.3	-0.5 ± 2.6	-0.10 ± 3.4
350	1.299	0.098 ± 0.076	0.088 ± 0.074	0.89 ± 0.28	22.6 ± 1.8	23.2 ± 1.8	10.9 ± 1.3	3.53 ± 0.43	3.15 ± 0.59
	1.278	0.060 ± 0.077	$-0.045 \pm .076$	0.12 ± 0.30	12 ± 2	14.8 ± 2.0	0.00 ± 1.9	-0.7 ± 0.7	-0.5 ± 0.8
360	1.976	0.059 ± 0.057	0.003 ± 0.058	0.43 ± 0.15	16.5 ± 1.3	11.5 ± 1.1	1.34 ± 0.61	0.55 ± 0.29	0.42 ± 0.30
	1.972	0.054 ± 0.058	-0.004 ± 0.058	0.33 ± 0.15	15.2 ± 1.4	10.5 ± 1.2	0.00 ± 0.86	0.03 ± 0.37	-0.01 ± 0.4
370	3.684	0.044 ± 0.028	0.002 ± 0.038	0.197 ± 0.092	17.9 ± 0.8	11.69 ± 0.57	1.49 ± 0.44	0.46 ± 0.17	0.41 ± 0.14
	3.676	0.039 ± 0.028	-0.003 ± 0.038	0.092 ± 0.097	16.47 ± 0.87	10.53 ± 0.66	0.00 ± 0.63	-0.12 ± 0.25	-0.08 ± 0.21
380	2.777	0.032 ± 0.045	-0.034 ± 0.041	0.034 ± 0.090	19.94 ± 0.75	11.56 ± 0.65	2.56 ± 0.63	0.89 ± 0.23	0.76 ± 0.29
	2.766	0.023 ± 0.046	0.023 ± 0.041	-0.15 ± 0.10	17.49 ± 0.97	9.58 ± 0.82	0.00 ± 0.90	-0.11 ± 0.34	-0.09 ± 0.36
390	0.231	0.71 ± 0.47	0.10 ± 0.42	2.91 ± 1.03	45.2 ± 7.1	55.0 ± 7.2	38.0 ± 6.6	18.8 ± 3.6	13.6 ± 2.9
	0.218	0.61 ± 0.50	-0.02 ± 0.44	0.22 ± 1.20	8.3 ± 10.2	26.5 ± 9.3	0.00 ± 9.9	4.3 ± 4.7	1.1 ± 3.9
400	0.008	1.01 ± 0.69	0.11 ± 0.71	34.8 ± 2.1	510 ± 17	541 ± 16	587 ± 18	261 ± 19	245 ± 11
	0.001	-9.4 ± 6.8	-16 ± 8	-62 ± 32	-595 ± 330	685 ± 144	0.00 ± 223	299 ± 77	464 ± 112
Total[c]	10.69	0.072 ± 0.026	0.032 ± 0.028	0.819 ± 0.083	25.53 ± 0.65	20.40 ± 0.67	10.5 ± 0.6	3.81 ± 0.26	3.22 ± 0.28
	10.52	0.035 ± 0.027	0.003 ± 0.028	0.074 ± 0.087	15.47 ± 0.75	12.31 ± 0.68	0 ± 0.62	0.26 ± 0.27	0.24 ± 0.29
Atmospheric Xe[d]		2.337	2.180	47.15	649.6	521.3	660.7	256.3	217.6

[a] Temperature of the crucible for stepped pyrolysis. Actual sample temperature may be several °C lower.

[b] Concentrations of ^{130}Xe based on total sample masses.

[c] Total composition is calculated by combining amounts of each isotope for all temperature fractions.
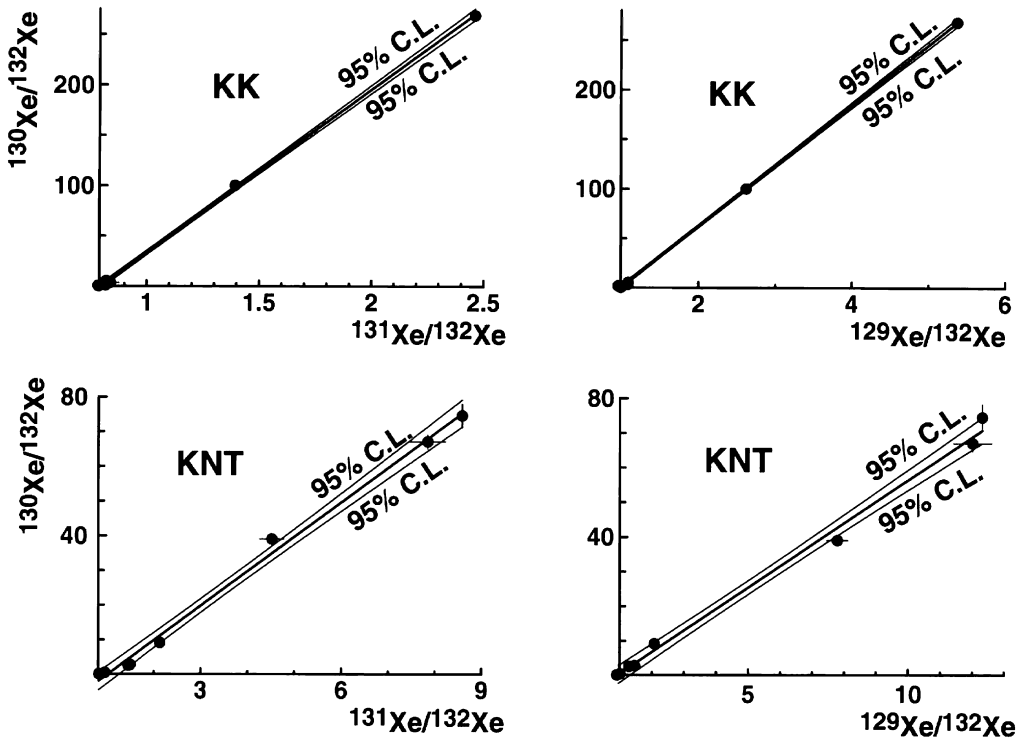
[d] Ref. [34].

Fig. 2a. Linear correlations between $^{129}Xe/^{132}Xe$, $^{131}Xe/^{132}Xe$ and $^{130}Xe/^{132}Xe$ released from Kalgoorlie krennerite (KK) and Kochbulak native tellurium (KNT) samples suggest a binary mixture with no measurable third, trapped Xe component.

it would appear as an apparent trapped component enriched in ^{130}Xe relative to atmospheric Xe composition. Fig. 2b shows the mixing lines in the vicinity of atmospheric Xe, the most diagnostic portion of the correlation lines for the composition of the trapped Xe. The value for the atmospheric $^{130}Xe/^{132}Xe$ ratio is 0.151, so all of the trapped compositions are atmospheric within uncertainty and we can then set the upper limits on quantity of parentless ^{130}Xe that could be present in these samples. Since there are two correlation lines, two limits for the apparent trapped Xe composition are obtained. For the Kochbulak sample, the trapped $^{130}Xe/^{132}Xe$ ratio is -1.95 ± 2.05 and 0.59 ± 2.10, for the krennerite it is -0.6 ± 2.4 and 0.3 ± 1.7 (from the $^{130}Xe/^{132}Xe$ vs. $^{131}Xe/^{132}Xe$ and the $^{130}Xe/^{132}Xe$ vs. $^{129}Xe/^{132}Xe$ correlations, respectively). By superimposing the upper limits from both plots, we constrain the maximal trapped $^{130}Xe/^{132}Xe$ to 0.2 for the Kochbulak and 2 for the Kalgoorlie sample. By comparing these limits to the average $^{130}Xe/^{132}Xe$ ratios (9.5 and 43.2, respectively) we set upper limits of $< 20\%$ and $< 5\%$ for the fractions of inherited (parentless) ^{130}Xe which could be present in these samples. But even these extreme upper limits are far too low to explain the "low" values of ^{130}Te DBDHL which would require that 60–70% of all the (non-atmospheric) ^{130}Xe to have been parentless ^{130}Xe trapped during formation of the Te minerals. Thus, this experiment effectively rules out inherited ^{130}Xe as an explanation for the "low" group of ^{130}Te $\beta\beta$ half-lives.
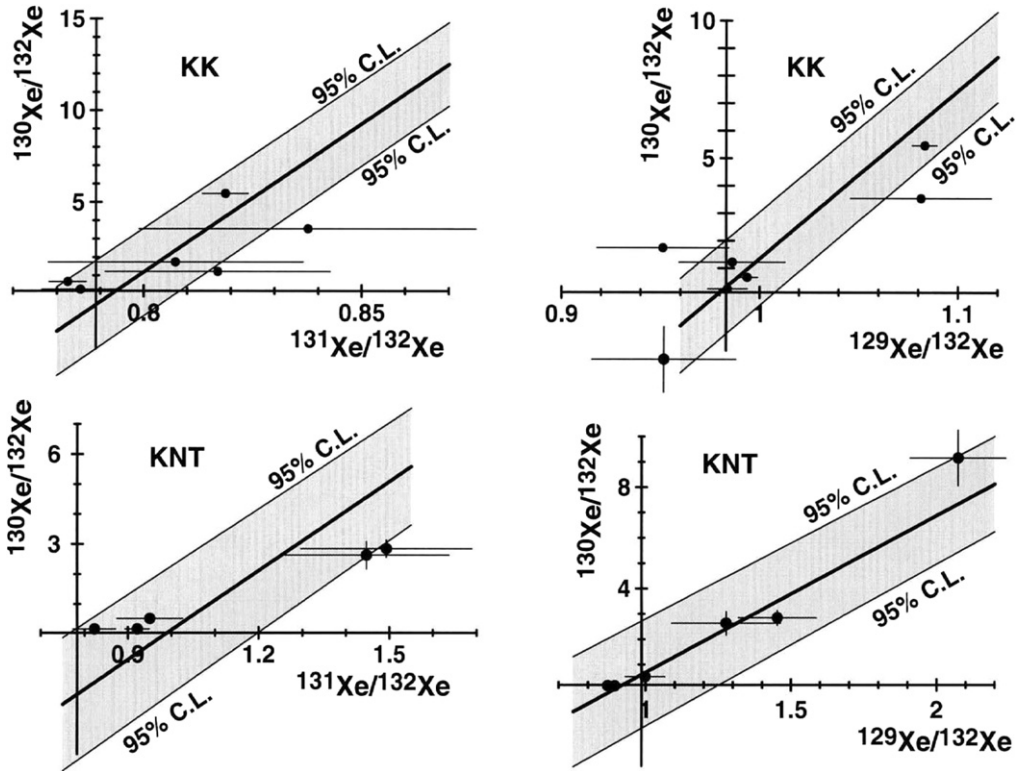
Fig. 2b. The enlarged parts of plots shown on Fig. 2a show the vicinity of atmospheric Xe (the origin of the axes) for the same samples (KK and KNT). The intersections with vertical axes show compositions of the trapped Xe component. The intersection with the +95% CL parabolas provide upper limits for these compositions.

3. Evaluation of problems with Xe retention

The most suitable samples for these experiments are old native Te specimens with the apparent ^{130}Te DBDHL belonging to the "high" DBDHL group. Metallic Te has a low melting point (hence low Tamman/Hüttig temperatures which define the onset of self-diffusion). We selected for this study the 1.6 Gyr Good Hope Mine sample of native Te, which previously yielded long ^{130}Te half-lives, as found independently in two different laboratories [2,9], and an American Mine sample of native Te, both from Colorado. These samples are both aliquots of the large specimens used earlier in DBDHL determinations [9,10,27], and are at least 99.9% pure polycrystalline Te as confirmed by SEM-EDX analyses.

If some ^{130}Xe has been partially lost from these samples during their long geologic histories, it probably diffused out along the grain boundaries or migrated with weakly-bound lattice defects. These types of losses should alter the distribution of the observed ^{130}Xe/^{130}Te ratios which should be higher and constant in undisturbed portions of the sample and relatively low in parts more affected by thermally-driven migration. Since mass spectrometers are better at measuring isotopic ratios than absolute quantities, it is less precise to measure the ^{130}Xe/^{130}Te ratios directly. We therefore irradiated our samples with thermal neutrons to convert some of the ^{130}Te to ^{131}I which decays to stable ^{131}Xe. Therefore, the *n*-capture-produced ^{131}Xe can be used

as a proxy for ^{130}Te, and any variation in the ^{130}Xe/^{130}Te ratio will be observed as variations in the ^{130}Xe/^{131}Xe ratio and accurately measured in our mass spectrometer. To extract xenon from different parts of the crystalline structure with different thermal properties for ^{130}Xe diffusion, we again used step-wise pyrolysis. At low extraction temperatures, gases begin to diffuse from the lower temperature sites, the weakly-bound defects and grain boundaries where preexisting $\beta\beta$ ^{130}Xe may have been subject to natural diffusive losses. If these losses did occur, the ^{130}Xe/^{131}Xe ratios will be lower at these temperatures. As the extraction temperature increases, the ratios will grow perhaps reaching a plateau indicating complete ^{130}Xe retention (no diffusive loss). These plateau values, if found, would imply a constant undisturbed ^{130}Xe/^{130}Te ratio which would correspond to the correct value for the $\beta\beta$ half-life. The wider the plateau, the smaller the amount of ^{130}Xe that was lost. A similar technique is routinely used in ^{40}Ar/^{39}Ar and ^{129}Xe/^{127}I dating, the so-called plateau ages, for minerals which have partially lost their noble gas decay products.

The Good Hope and American Mine native Te samples were irradiated by thermal neutrons at the University of Missouri–Rolla Reactor. Prior to irradiation they were sealed in evacuated (to $< 10^{-8}$ Torr) fused quartz capsules in order to measure and correct for any possible recoil losses of ^{131}Xe that occurred during irradiation. During the irradiation the sample package was constantly rotated in order to provide equal neutron fluence for each sample. Six months after irradiation, sufficient for most of 8d ^{131}I and 12d ^{131m}I to decay into ^{131}Xe, the gases were extracted by an 11-step step-wise pyrolysis (from 100 °C to 600 °C in increments of 20 °C to 60 °C, depending on details of the Xe release profile). Purification, separation from the light noble gases and mass spectrometric measurement were similar to those described in the previous experiment. The irradiation capsules were broken under vacuum in our sample system and any recoil-released Xe was analyzed, followed by the step-wise pyrolysis. The results are summarized in Table 2. For both samples, less than 0.03% of total ^{131}Xe was found to be in the gas phase, indicating negligible recoil effects. After the irradiation, ^{131}Xe is the dominant isotope, ~ 100 times the ^{130}Xe from $\beta\beta$-decay. While a small amount of ^{131}Xe may come from spontaneous ^{238}U fission and/or neutron-induced ^{235}U fission, this contribution is negligible, as indicated by the very small amounts of fission-produced ^{134}Xe and ^{136}Xe (Table 2). After subtraction of the trapped atmospheric contributions, the ratios of ^{130}Xe/^{131}Xe were determined as a function of the fractional release of ^{131}Xe as shown in Fig. 3. This plot clearly demonstrates a nearly constant ^{130}Xe/^{131}Xe ratio for all temperature fractions, implying that partial diffusive losses of ^{130}Xe were insignificant over the geologic history of these samples. If the "long" DBDHL were a result of partial ^{130}Xe losses, these losses must have be around 60–70%, amounts clearly ruled out by Fig. 3.

Therefore, the long half-lives for these samples could not be caused by incomplete ^{130}Xe retention, as was suggested by the low DBDHL proponents. Yet, it is hard to admit that both "short" and "long" values can be correct, with the apparent bimodality of ^{130}Te DBDHLs such as due to the (improbable) time-variability of the G_F^4 [19,20]. There clearly must be some other explanation.

The only possibility we have not yet considered is the *complete*, catastrophic loss of ^{130}Xe from these Te samples due to a singular event at a certain time in the past. This idea was first discussed by the Heidelberg group [2], although it was restricted to the 1.3 Gyr K–Ar age for Good Hope Mine and it was soon abandoned since there was no evidence for such geological events. It was believed that the last hydrothermal Te deposition in Colorado occurred ~ 1.6 Gyr ago [9,10,27], soon after the formation of the host rocks (~ 1.7 Gyr), with no secondary thermal episodes in the region. However, recent Ar–Ar thermochronological studies of the Colorado

Table 2

Concentration of ^{130}Xe and Xe isotopic composition of xenon (^{132}Xe $\equiv$ 100) released from neutron irradiated native tellurium samples during stepped pyrolysis. Second line in each extraction step shows residual composition after subtraction of atmospheric xenon contamination assuming all ^{132}Xe is due to air. Shown uncertainties are 1σ (68% CL). Negative ratios are due to overcorrection

Temp. (°C)[a]	^{130}Xe (10^{-12} cm^3 STP/g)[b]	^{124}Xe	^{126}Xe	^{128}Xe	^{129}Xe	^{131}Xe	^{132}Xe	^{134}Xe	^{136}Xe
276 mg *n*-irradiated Good Hope Mine native tellurium									
0	0.019	2.21 ± 0.55	2.79 ± 0.45	46.4 ± 2.9	657 ± 20	555 ± 21	667 ± 19	277 ± 9	240 ± 9
	< 0.000	15 ± 73	−65 ± 210	126 ± 400	−116 ± 3277	−3100 ± 11400	10 ± 2910	−2020 ± 7130	−2230 ± 7650
100	0.024	0.10 ± 0.28	0.66 ± 0.29	5.63 ± 0.65	71.65 ± 4.12	159 ± 9	66.8 ± 2.7	30.1 ± 1.7	27.1 ± 1.9
	0.022	−0.15 ± 0.31	0.48 ± 0.32	0.97 ± 0.75	6.6 ± 5.5	118 ± 10	0.00 ± 4.29	4.57 ± 2.2	5.5 ± 2.4
150	0.080	0.59 ± 0.12	0.46 ± 0.21	5.30 ± 0.46	71.6 ± 4.1	159 ± 9	66.9 ± 2.7	30.1 ± 1.7	27.1 ± 2.0
	0.072	0.40 ± 0.13	0.28 ± 0.22	0.99 ± 0.52	9.9 ± 3.2	75 ± 7	0.00 ± 2.19	2.0 ± 1.2	1.4 ± 1.2
200	0.049	0.25 ± 0.17	−0.29 ± 0.12	10.07 ± 0.56	133.6 ± 4.2	5248 ± 281	130.5 ± 3.1	63.9 ± 4.3	53.5 ± 1.9
	0.039	−0.26 ± 0.21	−0.90 ± 0.15	0.97 ± 0.75	6.6 ± 6.5	6409 ± 353	0.00 ± 5.55	16.5 ± 5.6	12.9 ± 2.6
250	0.076	0.51 ± 0.13	0.30 ± 0.11	7.37 ± 0.35	116.1 ± 3.5	1652 ± 44	108.6 ± 2.3	49.3 ± 1.7	46.9 ± 1.5
	0.064	0.15 ± 0.15	−0.07 ± 0.12	−0.44 ± 0.50	11.2 ± 5.0	1873 ± 53	0.00 ± 4.04	8.6 ± 2.3	13.3 ± 2.1
300	0.212	0.0244 ± 0.049	0.205 ± 0.053	5.43 ± 0.29	86.7 ± 3.4	4087 ± 164	76.6 ± 2.8	29.6 ± 1.2	25.9 ± 1.0
	0.187	−0.029 ± 0.057	−0.053 ± 0.061	−0.03 ± 0.39	12.78 ± 4.9	4554 ± 187	0.00 ± 4.49	−0.2 ± 1.8	0.7 ± 1.6
330	1.397	0.101 ± 0.015	0.098 ± 0.010	2.24 ± 0.08	42.23 ± 0.83	7978 ± 138	32.3 ± 0.3	13.1 ± 0.8	10.9 ± 0.4
	1.328	−0.014 ± 0.016	−0.009 ± 0.011	−0.06 ± 0.09	10.93 ± 0.94	8361 ± 145	0.00 ± 0.49	0.56 ± 0.86	0.29 ± 0.42
360	5.196	0.0135 ± 0.0016	0.0111 ± 0.0016	0.248 ± 0.012	16.84 ± 0.47	8723 ± 227	3.45 ± 0.06	1.31 ± 0.07	1.09 ± 0.04
	5.169	0.0014 ± 0.0016	−0.0003 ± 0.0016	0.002 ± 0.012	13.52 ± 0.47	8766 ± 229	0.00 ± 0.08	−0.032 ± 0.071	−0.049 ± 0.041
390	10.94	0.0066 ± 0.0012	0.0051 ± 0.0010	0.140 ± 0.009	14.72 ± 0.58	8400 ± 322	1.78 ± 0.05	0.656 ± 0.042	0.604 ± 0.036
	10.91	0.0003 ± 0.0012	−0.0007 ± 0.0010	0.014 ± 0.010	13.01 ± 0.58	8421 ± 324	0.00 ± 0.07	−0.034 ± 0.046	0.018 ± 0.040
410	5.515	0.0029 ± 0.0016	0.0045 ± 0.0012	0.078 ± 0.004	14.01 ± 0.53	8356 ± 311	0.771 ± 0.020	0.397 ± 0.049	0.347 ± 0.015
	5.509	0.0002 ± 0.0016	0.0020 ± 0.0012	0.023 ± 0.005	13.26 ± 0.53	8365 ± 312	0.00 ± 0.029	0.098 ± 0.050	0.093 ± 0.016
450	0.008	0.05 ± 0.56	0.25 ± 0.73	16.2 ± 1.6	441 ± 24	5848 ± 381	226.9 ± 8.1	113 ± 11	116 ± 13
	0.006	−1.14 ± 0.85	−0.76 ± 1.11	0.01 ± 2.58	332 ± 37	8630 ± 560	0.00 ± 17.5	38 ± 17	63 ± 20
500	0.006	0.34 ± 1.05	0.1 ± 1.15	22.7 ± 2.1	337 ± 19	4756 ± 275	348 ± 18	187 ± 12	174 ± 11
	0.003	−1.87 ± 2.23	−2.05 ± 2.44	−4.3 ± 5.3	−11 ± 55	9460 ± 774	0.00 ± 53.6	110 ± 28	125 ± 23
600	0.005	3.3 ± 4.6	0.3 ± 2.5	18.2 ± 5.8	447 ± 54	2446 ± 338	388 ± 42	214 ± 29	207 ± 30
	0.002	4.7 ± 11.2	−2.2 ± 6.0	−23 ± 18	158 ± 150	5184 ± 1090	0.00 ± 145	154 ± 73	191 ± 72
Total[c]	23.53	0.0218 ± 0.0019	0.0186 ± 0.0016	0.443 ± 0.013	18.98 ± 0.35	8322 ± 174	6.09 ± 0.15	2.505 ± 0.082	2.181 ± 0.060
	23.31	0.0003 ± 0.0020	−0.001 ± 0.003	0.009 ± 0.010	13.12 ± 0.33	8395 ± 176	0.000 ± 0.067	0.144 ± 0.094	0.174 ± 0.086

Table 2 (*continued*)

Temp. (°C)[a]	130Xe (10⁻¹² cm³ STP/g)[b]	124Xe	126Xe	128Xe	129Xe	131Xe	132Xe	134Xe	136Xe
173.3 mg *n*-irradiated American Mine native tellurium									
0	0.4934	2.44 ± 0.11	2.391 ± 0.098	46.28 ± 0.66	639 ± 9	685 ± 8	650 ± 6	253 ± 3	216 ± 3
	0.0084	8.4 ± 7.3	14.9 ± 9.1	−0.6 ± 48	−2 ± 625	10162 ± 53	0 ± 520	58 ± 205	83 ± 170
150	0.0304	0.69 ± 035	1.10 ± 0.55	39.8 ± 3.2	541 ± 39	975 ± 72	552 ± 39	222 ± 16	197 ± 14
	0.0050	−7.6 ± 4.1	−4.23 ± 4.01	2.8 ± 25.2	−9 ± 330	3267 ± 1166	0 ± 331	45 ± 124	94 ± 98
200	0.0445	2.59 ± 0.37	2.02 ± 0.41	379 ± 1.4	535 ± 14	2013 ± 53	540 ± 12	220 ± 7	180 ± 5
	0.0081	3.7 ± 2.0	1.3 ± 2.2	−3.2 ± 9.4	24 ± 100	8657 ± 548	0 ± 93	56 ± 42	10 ± 36
250	0.0652	1.39 ± 0.20	1.20 ± 0.36	30.6 ± 1.2	412 ± 9	6892 ± 169	420 ± 7	169 ± 5	143 ± 4
	0.0238	−0.24 ± 0.56	−0.5 ± 1.0	2.0 ± 3.6	0.6 ± 32	179657 ± 708	0 ± 29	16 ± 14	12 ± 13
300	0.2896	0.318 ± 0.062	0.228 ± 0.043	8.50 ± 0.32	111 ± 3	10258 ± 307	112 ± 3	44.6 ± 1.3	38.4 ± 1.0
	0.2406	−0.09 ± 0.08	−0.17 ± 0.05	0.65 ± 0.44	1.65 ± 4.7	12238 ± 375	0.0 ± 4.5	1.49 ± 1.97	1.8 ± 1.6
330	1.005	0.152 ± 0.020	0.166 ± 0.018	3.143 ± 0.09	43.55 ± 0.71	11264 ± 225	43.32 ± 0.62	17.46 ± 0.35	15.39 ± 0.29
	0.939	−0.01 ± 0.02	0.026 ± 0.019	0.05 ± 0.11	1.0 ± 1.0	12017 ± 241	0.0 ± 0.9	0.72 ± 0.46	1.2 ± 0.4
360	3.322	0.0275 ± 0.0049	0.0331 ± 0.0038	0.616 ± 0.019	8.91 ± 0.20	10892 ± 486	8.13 ± 0.16	3.193 ± 0.082	2.881 ± 0.072
	3.281	−0.001 ± 0.005	0.0064 ± 0.0038	0.038 ± 0.022	0.92 ± 0.26	11021 ± 492	0.00 ± 0.23	0.04 ± 0.11	0.20 ± 0.09
390	8.339	0.0137 ± 0.0032	0.0164 ± 0.0032	0.366 ± 0.019	5.28 ± 0.23	10892 ± 465	4.63 ± 0.19	1.96 ± 0.10	1.707 ± 0.090
	8.281	−0.0026 ± 0.0033	0.0012 ± 0.0033	0.037 ± 0.024	0.73 ± 0.30	10687 ± 468	0.00 ± 0.28	0.12 ± 0.13	0.09 ± 0.11
420	7.163	0.372 ± 0.016	0.361 ± 0.041	7.56 ± 0.14	94.6 ± 1.7	8971 ± 2.18	94.9 ± 1.7	38.75 ± 0.91	33.96 ± 0.76
	6.135	0.044 ± 0.019	0.056 ± 0.048	0.35 ± 0.22	1.5 ± 2.8	10386 ± 257	0.0 ± 2.8	2.2 ± 1.3	3.1 ± 1.1
450	1.033	1.909 ± 0.099	2.110 ± 0.075	39.89 ± 0.44	544 ± 17	2014 ± 14	555 ± 3	241.2 ± 3.7	211 ± 5
	0.1653	−0.32 ± 0.63	1.76 ± 0.48	2.1 ± 3.2	−13 ± 110	9842 ± 317	0 ± 31	163 ± 24	177 ± 33
500	0.558	2.20 ± 0.12	2.096 ± 0.091	42.35 ± 1.0	620 ± 29	1631 ± 35	620 ± 12	253 ± 5	219 ± 5
	0.0345	0.2 ± 2.0	0.9 ± 1.5	−29 ± 28	161 ± 496	18453 ± 5379	0 ± 280	203 ± 88	236 ± 77
600	0.0227	1.92 ± 0.48	0.80 ± 0.55	43.0 ± 2.1	611 ± 18	1313 ± 47	622 ± 16	256 ± 8	252 ± 41
	0.0013	−4.8 ± 8.6	−22 ± 13	−23 ± 45	−23 ± 408	1395 ± 5444	0 ± 375	243 ± 141	802 ± 744
Total[c]	22.37	0.348 ± 0.011	0.349 ± 0.016	6.92 ± 0.16	95.3 ± 2.4	9263 ± 203	95.9 ± 2.2	39.52 ± 0.93	34.41 ± 0.83
	19.12	0.0116 ± 0.0103	0.0396 ± 0.0174	0.111 ± 0.096	1.20 ± 1.63	1074 ± 235	0.0 ± 1.1	2.71 ± 0.53	3.24 ± 0.52
Atmospheric Xe[d]		2.337	2.180	47.15	649.6	521.3	660.7	256.3	217.6

[a] Extraction temperature for stepped pyrolysis. The 0 °C data are for Xe found in the irradiation capsule.
[b] Concentrations of 130Xe based on total sample masses (assuming that the samples are 100% pure Te). The uncertainties on these values are ~ 7% due to reproducibility of known standard amount of atmospheric Xe daily admitted to the mass-spectrometer to determine sensitivity and mass-discrimination.
[c] Total composition is calculated by combining amounts of each isotope for all temperature fractions including gas in the capsule.
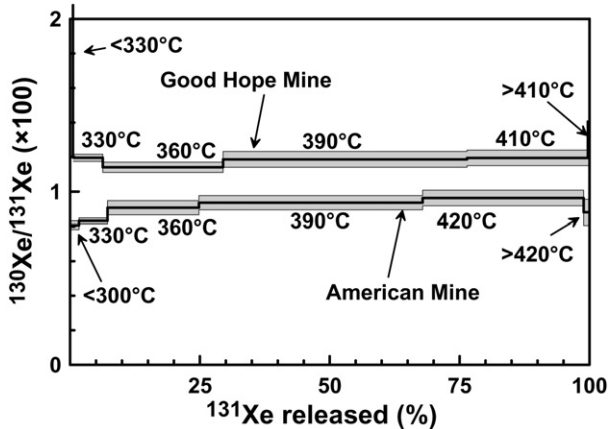[d] Ref. [34].

Fig. 3. Plateau plots demonstrate excellent ^{130}Xe retention: $\sim 95\%$ in the American Mine and $\sim 100\%$ in the Good Hope Mine. The vertical thickness of the lines represents 2 standard deviations.

Front Range have revealed multiple metamorphic episodes from 1.4 to 1.34 Gyr with peak temperatures exceeding $\sim 525\,°C$ [28], well above the Te melting point of $452\,°C$. Such episodes would completely degas these native Te samples, but not affect the Pb ages (1.66 and 1.60 Gyr, respectively, for the American and Good Hope Mines [9,10]). The reconstructed average cooling path for Northern and Central Colorado Front Rage suggests that even much later, ~ 750 Myr ago, the temperature was still between 150 and $200\,°C$ [29]. Furthermore, some growing, but not yet conclusive evidence suggests that early in the Paleozoic (~ 570 Myr ago) a slow thermal buildup beneath Rodinia, the first proported global supercontinent incorporating essentially all the Earth's continents, caused the old continental crust to dome, stretch, weaken and eventually rupture. Was this the event that degassed the older Te samples, those that provide the longer apparent DBDHL? We do not know, but the Early Paleozoic is the right time to "shift" apparent ^{130}Te DBDHL from the "long" to the "short" group of DBDHL values. If this is the explanation, Xe must have escaped from these native Te samples below the melting point of Te. To address this question we conducted an experiment to explore Xe diffusion in native tellurium samples at sub-liquidous temperatures.

4. Xe diffusion in Te

To study Xe mobility in Te at prolonged sub-liquidous temperatures, ~ 20 mg aliquots of the American Mine native Te sample were held at $260\,°C$ for 68 and 244 days. These Te samples were then loaded into the vacuum system and subjected to step pyrolysis with subsequent mass spectrometric analysis of xenon released from each temperature step. After the normal corrections for mass-discrimination ($\sim 0.2\%$/amu) and minor atmospheric contamination, the cumulative ^{130}Xe releases were plotted as functions of the extraction temperature (Fig. 4). Significant ^{130}Xe losses from the lower temperature fractions occurred for the Te samples kept at $260\,°C$ even after only a few months. These losses also depend on the diffusion distance, as evident from comparison of the release pattern from a powdered native Te with an uncrushed aliquots (Fig. 4), suggesting that the losses are volume dependent, thus probably not due to defect mobility or grain-surface effects, but to conventional thermal diffusion.

The tellurium sample held at $260\,°C$ for 68 days lost 4.7% of ^{130}Xe, while 244 days at the same temperature caused $\sim 11\%$ losses. According to thermal diffusion theory, the fraction of
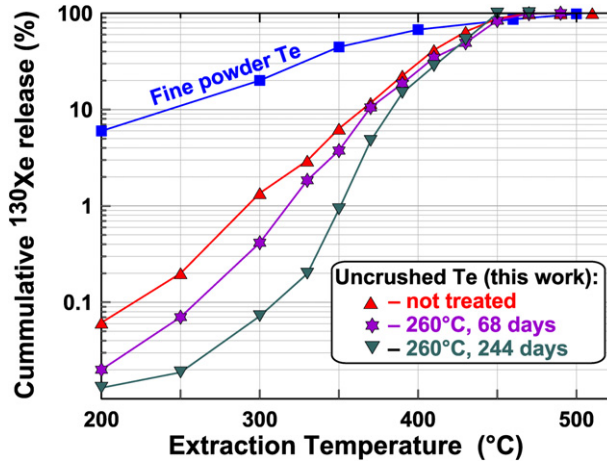
Fig. 4. Cumulative ^{130}Xe release profiles from the American Mine native Te—one aliquot of untreated Te powder [27] and three aliquots of uncrushed Te (one unheated and two held at 260 °C for two different time periods). Each extraction temperature step lasted for 45 minutes, sequentially degassing the more retentive sites.

loss is proportional to the square root of diffusion time for any given geometry. Using the numbers obtained, we independently estimated this factor to be 10.9% yr$^{-1/2}$ and 13.5% yr$^{-1/2}$. This implies that, if the American Mine native Te were kept at 260 °C for less than 100 years (between 54 and 83 yr, to be more precise), it would loose at least 99% of its radiogenic ^{130}Xe. One century is short on the geological time scale, and 260 °C is a mild temperature for such geothermal events as the rupture of the supercontinent Rodinia, if it indeed took place or some other mild geothermal excursions undetected by conventional methods. The problem with confirming any such scenario is that present-day radiometric dating techniques are not as sensitive to such mild thermal events and cannot provide direct chronometric evidence for it.

5. Geochronology of Te ores

Native tellurium samples themselves do not contain any elements which can be directly used as a chronometer. Most of the reported long ^{130}Te DBDHLs [9,10,27] are based on Xe retention ages estimated from the Stacey–Kramers model for two-stage evolution of global Pb [30]. This model relies heavily on several hard-to-verify assumptions and, according to the authors of this model, "can only be an approximation" and there is no consensus about how reliable these common Pb model ages are. Moreover, they are sensitive only to Pb mobility, not Xe mobility in metallic Te. Nevertheless, one study concluded "there is no reason to challenge the interpretation that the ore [native Te] formed at essentially the same time as their host rocks" [10]. But in our case it is not the formation age of the host rock that is important, but the Xe retention age. These two ages will be the same only if Te samples remained cool enough to arrest Xe diffusion and undisturbed since their formation 1.7 Gyr ago. Common geological knowledge states, however, that "it is almost impossible to find geologically old minerals which never experienced at least mild 200–300 °C metamorphic episodes at later times" [31]. Such low temperature events will not affect conventional isotope chronometers but, as we have demonstrated, they will reset the Te–Xe clock. Therefore, considering the results of our diffusion experiments

(Fig. 4), Paleozoic geological events that likely occurred can easily cause a complete Xe loss from native Te, resetting the Xe retention clock which results in incorrect and anomalously long DBDHLs.

6. Fission xenon

It may be very tempting to consider using the accumulated fission-produced $^{136-132}$Xe to measure the Xe retention age of native Te since, regardless of whether the origin is from uranium fission or ^{130}Te, all Xe isotopes have the same diffusion properties. Fig. 5 shows the composition of heavy Xe isotopes (data from Table 3 renormalized to ^{132}Xe) released from the American and Good Hope Mine native Te samples. Also shown are directions to Xe produced in ^{235}U and ^{238}U fissions. The composition of the heavy Xe isotopes is close to that of atmospheric Xe with only small additions of Xe from ^{238}U fission and even smaller additions from ^{235}U fission (if any). Interestingly, the Xe released at high temperatures is notably enriched in fission Xe. For both American and Good Hope Mines the ^{134}Xe/^{132}Xe and ^{136}Xe/^{132}Xe ratios reach their maximal values at 450, 500, and 600 °C, above the melting point of metallic Te, while major release of Te-derived ^{130}Xe occurs below 400 °C. This suggests that the carrier of fission Xe is not Te, but some more refractory U-bearing inclusions in the native Te matrix. These inclusions are probably very small and easily overlooked by the SEM-EDX technique used to establish the purity of these native Te samples. The detection limit of this technique is only about 0.1% and 10 keV electrons do not penetrate very far into a metallic Te sample, thus SEM-EDX only provides information within ∼ 1 µm of the surface.

The uranium contents measured in several 5–10 mg aliquots of both Good Hope and American Mine tellurium samples using a ICP-MS technique were poorly reproducible, ranging from 0.1 to ∼ 30 ppb, while the analyses of reference U standards varied by < 10%, suggesting heterogeneity in the U distribution, as expected from such U-bearing inclusions. Table 3 summarizes analyses of Good Hope Mine tellurium made in several different laboratories. While concentrations of Te-derived ^{130}Xe are nearly constant, the fission Xe contents vary dramatically. U-contents determined from analyses of sub-samples of the Good Hope Mine Te are also not reproducible. All of these observations suggest that U is present in these native Te samples not as a solid solution, but concentrated in accessory mineral inclusions. The same conclusion was reached from Xe analyses. Since the fission Xe is most pronounced at extraction temperatures above melting point of Te (Fig. 5), it cannot be located in the metallic tellurium, but hosted in inclusions within the sample. It is likely that 600 °C, the highest temperature used in this study, was too low to extract all fission Xe from inclusions (most silicates melt at > 1100 °C). Thus we conclude that ^{238}U–^{136}Xe ages, if they can be interpreted at all, do not have any bearing upon the Xe retention age of these samples.

Since Pb ages were used only for geologically old (> 1 Gyr) Te samples [9,10,27], the ^{130}Te DBDHLs computed for these samples are probably overestimated, resulting in the apparent bimodal grouping between DBDHLs for old samples and young samples. In this context the geologically young and the more thermally pristine samples provide the more reliable ^{130}Te DBDHLs. Thus, we have solved the mystery. It is not inherited ^{130}Xe, it is not partial diffusive losses of ^{130}Xe and it is not a temporal evolution of the Fermi constant [19,20] but it is the singular and significant thermal events that completely reset the Xe retention ages and produced the anomalously high apparent $\beta\beta$ half-lives of ^{130}Te in the older samples and the observed bimodal pattern.
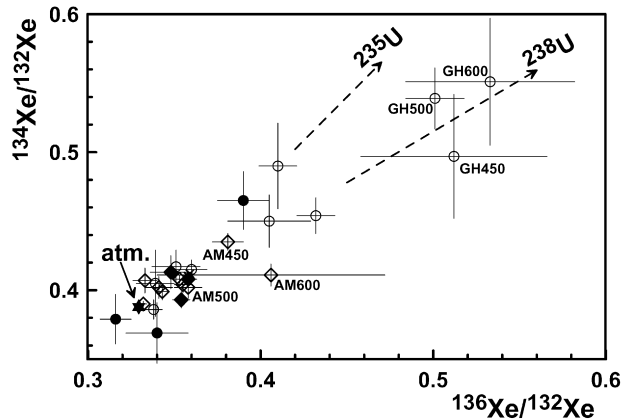
Fig. 5. Heavy Xe isotopes in American Mine (diamonds) and Good Hope Mine (circles) native tellurium samples. Also shown are atmospheric composition (atm.) and the directions to fission products from ^{235}U and ^{238}U. Numbers after sample abbreviations (AM or GH) are extraction temperatures in °C. Filled symbols correspond to the richest ^{130}Xe extractions. In both samples, the highest temperature extractions tend to contain more fission contributions.

Table 3
Xenon and uranium concentrations in Good Hope Mine native tellurium. Concentrations of ^{130}Xe from ^{130}Te $\beta\beta$-decay, ^{132}Xe from ^{238}U fission and total ^{132}Xe (consisting mainly of atmospheric Xe) are shown in units of 10^{-13} cm^2 STP/g Te. These Xe components were determined by deconvolution of Xe isotope analyses made from the same Te samples. Uranium analyses (in part per billion) were made in aliquots of these samples and evident scatter of uranium content and fission xenon concentration and the absence of the correlation between the two suggest inhomogeneous sampling

Reference and sample number and source	Weight (g)	^{130}Xe	Total ^{132}Xe	Fission ^{132}Xe	U content (ppb)
Kirsten et al., 1968 (#98589, HUMM) [2]	0.866	240 ± 40	31.7	Not found	21 ± 2
Richardson et al., 1986 (#98589A, HUMM) [14]	0.3468	275 ± 17	35.5	0.36	Not determined
Bernatowicz et al., 1993 (#85138, NMNH) [27]	2.9988	234 ± 12	9.6	0.01	2.6, 3.3 (repeat analyses)
This work (#85138, NMNH)	0.2760	233 ± 16	14.3	0.27	29, 0.5, 10, 1.3 (independent analyses)
This work (#R181, USNM)	0.0896	224 ± 16	8.3	0.05	35

HUMM = Harvard University Mineralogical Museum, NMNH = National Museum of Natural History, USNM = US National Museum (Division of Mineralogy).

7. Best current estimate for ^{130}Te and ^{128}Te DBDHLs

Our experiments suggest that complete Xe losses occur in native Te at modest temperatures documented in known secondary geothermal episodes. Pb geochronology, previously considered a reliable measure of Xe accumulation time [9,10,27], is decoupled from and insensitive to Xe losses from native Te in these events and, therefore, not a reliable measure of the ^{130}Xe retention time. Geologically young samples, which tend to yield smaller ^{130}Te DBDHL values, are therefore the more reliable because they are less likely to have experienced significant post-

formational geothermal episodes. On the other hand, only old Te-samples with minimal neutron exposure are suitable for accurate determination of the ^{128}Te DBDHL but, since this is done by means of the ratio of ^{128}Xe to ^{130}Xe from the $\beta\beta$-decay of ^{128}Te and ^{130}Te [9], it is independent of such losses.

The best candidate method for the direct measurement of gas-retention ages of Te minerals is double beta decay itself. As it was proposed by the Heidelberg group 22 years ago [8], this can be done by utilizing the ^{82}Se $\to$ ^{82}Kr, as a Kr and Xe-retention chronometer. Since the ^{82}Se DBDHL is relatively well established ($1.0–1.3 \times 10^{20}$ yr, the entire range of published values), and there are minerals that contain both Se and Te, the accumulation of ^{82}Kr can, in principle, provide a reliable Xe-retention age with only one potential problem, the preferential loss of Kr relative to Xe. However, as we have demonstrated (and previously pointed out [14]), Xe losses, if they occur, are usually complete so Xe retentivity would be reflected in Kr retentivity. The ^{130}Te DBDHL calculated from analyses of kitkaite (NiTeSe) [15] falls right in the middle of "short" DBDHL values, lending strong support to the cluster of "short" DBDHL of ^{130}Te as the correct value. We therefore propose that the ^{130}Te DBDHL should be $9.0 \pm 1.4 \times 10^{20}$ yr (as the weighted average of [11–18]) and ^{128}Te DBDHL should be $2.41 \pm 0.39 \times 10^{24}$ yr (corresponding to the observed ratio of ^{128}Te-derived ^{128}Xe to ^{130}Te-derived ^{130}Xe of $3.74 \pm 0.10 \times 10^{-4}$ [32]).

Note added

One week after this paper was submitted for publication, the NEMO-3 Collaboration released a preliminary result from 534 days of counting estimating a direct measurement of the ^{130}Te half life to be $7.6 \pm 1.5(\text{stat}) \pm 0.8(\text{syst}) \times 10^{20}$ yr [33], in good agreement with our value of $9.0 \pm 1.4 \times 10^{20}$ yr.

Acknowledgements

References

[1] M.G. Inghram, J.H. Reynolds, Phys. Rev. 78 (1950) 822.
[2] T. Kirsten, O.A. Schaeffer, E. Norton, R.W. Stoenner, Phys. Rev. Lett. 20 (1968) 1300.
[3] E.C. Alexander Jr., B. Srinivasan, O.K. Manuel, Earth Planet. Sci. Lett. 5 (1968) 478.
[4] B. Srinivasan, E.C. Alexander Jr., O.K. Manuel, Econ. Geol. 67 (1972) 592.
[5] B. Srinivasan, E.C. Alexander Jr., O.K. Manuel, J. Inorg. Nucl. Chem. 34 (1972) 2381.
[6] T. Kirsten, AIP Conf. 96 (1983) 396.
[7] T. Kirsten, H. Richter, E. Jessberger, Phys. Rev. Lett. 50 (1983) 474.
[8] T. Kirsten, E. Heuser, D. Kaether, J. Oehm, E. Pernicka, M. Richter, in: T. Kotani, H. Ejiri, E. Takasugi (Eds.), Nuclear Beta Decays and the Neutrino, World Scientific, Singapore, 1986, p. 81.
[9] T. Bernatowicz, J. Brannon, R. Brazzle, R. Cowsik, C. Hohenberg, F. Podosek, Phys. Rev. Lett. 69 (1992) 2341.
[10] F.A. Podosek, J.C. Brannon, T.J. Bernatowicz, R. Brazzle, R. Grauch, R. Cowsik, C.M. Hohenberg, in: J. Matsuda (Ed.), Noble Gas Geochemistry and Cosmochemistry, Terra Scientific Publishing Co., 1994, p. 89.
[11] N. Takaoka, K. Ogata, Z. Naturforsch. 21a (1966) 84.

[12] E.W. Hennecke, O.K. Manuel, Phys. Rev. C 11 (1975) 1378.
[13] O.K. Manuel, in: T. Kotani, H. Ejiri, E. Takasugi (Eds.), Nuclear Beta Decays and the Neutrino, World Scientific, Singapore, 1986, p. 71.
[14] J.F. Richardson, O.K. Manuel, B. Sinha, Nucl. Phys. A 453 (1986) 26.
[15] W.J. Lin, O.K. Manuel, G.L. Cummings, D. Krstic, R.I. Thorpe, Nucl. Phys. A 481 (1988) 477.
[16] K.Y. Chiou, O.K. Manuel, in: S. Kato, T. Ohshima (Eds.), Proceedings of the XVI INS Int. Symposium: Neutrino and Related Topics, World Scientific, Singapore, 1988, p. 178.
[17] N. Takaoka, Y. Motomura, K. Nagao, Phys. Rev. C 53 (1996) 1557.
[18] J.D. Gilmour, R.A. Pattrick, G. Turner, D.I. Groves, P. McConville, in: C.J. Stanley, et al. (Eds.), Mineral Deposits: Processes to Processing, ISBN 90 5809 068 X (1999) 1259.
[19] A.S. Barabash, Phys. At. Nucl. 63 (2000) 1210.
[20] A.S. Barabash, Astrophys. Space Sci. 283 (2003) 607.
[21] R. Arnold, et al., Nucl. Phys. A 658 (4) (1999) 299.
[22] S.V.S. Murty, K. Marti, Geochim. Cosmochim. Acta 51 (1987) 163.
[23] W.J. Lin, O.K. Manuel, L.L. Oliver, Nucl. Phys. A 457 (2) (1986) 285.
[24] A.P. Meshik, C.M. Hohenberg, O.V. Pravdivtseva, Y.S. Kapusta, Phys. Rev. C 64 (2001) 035205.
[25] V.A. Kovalenker, Yu.G. Safonov, B.V. Naumov, V.L. Rusinov, Geologia Rudnykh Mesporozhdenii 39 (1997) 127 (in Russian), ISSN: 0016-7770. Also: www.igem.ru/igem/ored/kovlnkr.htm.
[26] N.N. Baranova, A.B. Vlynskii, S.V. Kozerenko, V.A. Kovalenker, V.P. Kolotov, N.N. Kolpakova, Geochimiya 12 (1995) 786, ISSN: 0016-75251.
[27] T. Bernatowicz, J. Brannon, R. Brazzle, R. Cowsik, C. Hohenberg, F. Podosek, Phys. Rev. C 47 (1993) 806.
[28] C.A. Shaw, L.W. Snee, J. Silverstone, J.C. Reed Jr., J. Geol. 107 (1999) 49.
[29] S. Marshak, K. Karlstrom, J.M. Timmons, Geology 28 (2000) 735.
[30] J.S. Stacey, J.D. Kramers, Earth Planet. Sci. Lett. 26 (1975) 207.
[31] L.A. Neymark, personal communication, US Geological Survey, Box 25046, MS963, Denver, CO 80225.
[32] M.T.F. da Cruz, et al., Phys. Rev. C 48 (1993) 3106.
[33] A.S. Barabash, NEMO-3 double beta decay experiment: Last results, in: Carolina International Symposium on Neutrino Physics, 15–17 May 2008, http://www.physics.sc.edu/CISNP/program.htm.
[34] M. Ozima, F. Podosek, Noble Gas Geochemistry, second ed., Cambridge Univ. Press, 2002, p. 286.